

MULTIFUNCTIONAL COMPOSITES REINFORCED WITH FUNCTIONALIZED NANOMATERIALS: INTERPHASE CHARACTERIZATION AND APPLICATIONS

Qi An¹, Andrew N. Rider², Narelle Brack³ and Erik T. Thostenson⁴

¹Center for Composite Materials, University of Delaware
101 Academy Street, Newark, DE 19716, United States
Email: qian@udel.edu

²Air Vehicles Division, Defence Science and Technology Organization
Fisherman's Bend, Victoria 3207, Australia
Email: andrew.rider@dsto.defence.gov.au

³Department of Chemistry and Physics, La Trobe University
Melbourne, Victoria 3086, Australia
Email: n.brack@latrobe.edu.au, web page: <http://www.latrobe.edu.au/physics>

⁴Department of Mechanical Engineering, University of Delaware
126 Spencer Laboratory, Newark, DE 19716, United States
Email: thosten@udel.edu, web page: <http://research.me.udel.edu/thostens/>

Keywords: Multifunctional nanocomposites, Carbon nanotubes, Electrophoresis,
Interphase, Shear strength

ABSTRACT

The current research explores a novel and industrially scalable processing technique to hybridize carbon nanotubes with traditional advanced fibers to prepare composites with multifunctional capabilities. High concentrations of carbon nanotubes (CNTs) have been integrated in fibrous preforms using an electrophoretic deposition (EPD) approach to produce composite materials with improved structural and functional performance. A stable aqueous dispersion of CNTs was produced using a novel ozonolysis and ultrasonication (USO) technique that results in dispersion and functionalization in a single step. Within the composite, networks of CNTs span between adjacent fibers, and the resulting composites exhibit significant increases in electrical conductivity and considerable improvements in the interlaminar shear strength and fracture toughness. In order to better understand the underlying mechanisms behind the selective reinforcement of CNTs on the glass-epoxy systems, model interphases were created on planar glass substrates and the surface chemistry and mechanical performance was characterized. The glass substrates were modified with a silane coupling agent followed by deposition of ozone and PEI functionalized CNTs. Lap shear joints were fabricated to examine the model interphase shear strength. Mechanical testing provided relative shear strength and failure representative of that occurring in a fiber composite. Chemical characterization of the failure surfaces using high resolution X-ray photoelectron spectroscopy (XPS) indicated increased shear strength occurred when fracture propagated in the CNT-rich interphase region between the glass and resin. Additionally, preliminary microdroplet debond tests have been conducted to investigate the interfacial properties between an epoxy matrix and E-glass fibers with the electrophoretically coated CNTs. The CNT-modified glass-fiber composites also exhibited electrical-resistance sensitivity to applied shear strain, with the rate of change dependent on the extent of plastic deformation, which enables damage sensing and structural health monitoring applications. The USO technique has also been applied to processing of exfoliated graphite and has enabled EPD of graphitic nanoplatelets onto E-glass fibers.

1 INTRODUCTION

As internal stress transfer in composites occurs at the interface, mechanisms of fiber/matrix adhesion are of fundamental scientific and technical interest as they strongly influence the ultimate strength of the composite [1]. A growing body of work [2-4] indicates that it should be possible to tune the level of adhesion at the fiber/resin interface by controlling both the heterogeneity of surface morphology and chemical reactivity. The success in composite design depends on controlling these interfacial properties to achieve the desired macroscopic material property for a given application.

Nanomaterials have been proven to have unique chemical, mechanical and physical properties, and therefore have a wide array of applications, especially in the field of composites [5-8]. Improved interfacial shear strength of glass fiber/epoxy composites investigated using fiber push-out microindentation was achieved by dispersing CNTs in the fiber sizing formulation or the matrix [5]. Percolating carbon nanotube networks dispersed in sizing was used to sense *in situ* damage of fiber reinforced polymer composites [6]. Thermal properties can also be enhanced by incorporating CNTs into composites using electrophoretic deposition [7]. It been shown that by hybridizing carbon nanotubes with carbon fibers the interfacial shear strength can be increased from about 65 to 126 MPa [8]. The integration of nanomaterials in composites can be utilized to impart new functionality to existing advanced composite material systems.

While many of these applications prove the unique enhancements nanomaterials offer, these studies often neglect to study the interface region of these composites. Some of the studies are theoretically based [9, 10], creating high fidelity models of the interface region. However, due to the complex nature of the interphase region modified with nanomaterials, it is often difficult to design experiments that can confirm the specific interactions examined in the models. For a similar reason, most practical engineering models of composite structures do not include the influence of nanoscale interactions on macro-scale mechanical properties [11-13]. While incorporating CNTs into composite materials has shown some improvements, some techniques may lead to degradation of the fiber properties. For example, chemical vapor deposition – a high temperature technique used to grow CNTs directly onto the fiber surfaces – can degrade the fiber strength and modulus if conditions and fiber pretreatments are not considered [8].

Electrophoretic deposition (EPD) is a widely used industrial coating process that has the benefits of low energy use and the ability to homogeneously coat a variety of practical materials with high density coatings [14-16]. EPD involves a two-step process in which the charged particles in solution move between an applied electric field and then deposit onto the electrode surface, forming a film. Successful EPD relies on the functionalization of the dispersed material, which enables a surface charge to develop. The surface charge, or zeta-potential, is dependent on the solution pH and helps to aid dispersion and mobility under applied electric fields [17-20]. The EPD process has in the benefit that the deposition may be carried-out under ambient conditions and allows for manipulation of the nanomaterial chemistry for the specific application.

Our recent research has applied this efficient EPD process for depositing functionalized CNTs onto conductive carbon fiber [21] and nonconductive glass fiber substrates [22]. Similar techniques have also been extended to processing of exfoliated graphite which has enabled EPD of graphitic nanoplatelets onto E-glass fibers, as shown in Figure 1, as well as preparation of aqueous dispersions that are suitable for ink-jet printing applications [23]. The significant improvements observed from the EPD-CNT reinforced fiber/epoxy composites are believed to be due to the CNTs modifying the interphase properties, leading to the fracture path moving away from the matrix/fiber interface and into the CNT-rich interphase region. The current research focuses on understanding the influence of CNT functionalization on the composite interphase chemistry and how this then affects the macroscale mechanical performance of the laminate. Both model interphase [24] and interface characterizations at the single fiber level are being undertaken to establish the relative contributions to composite mechanical performance.

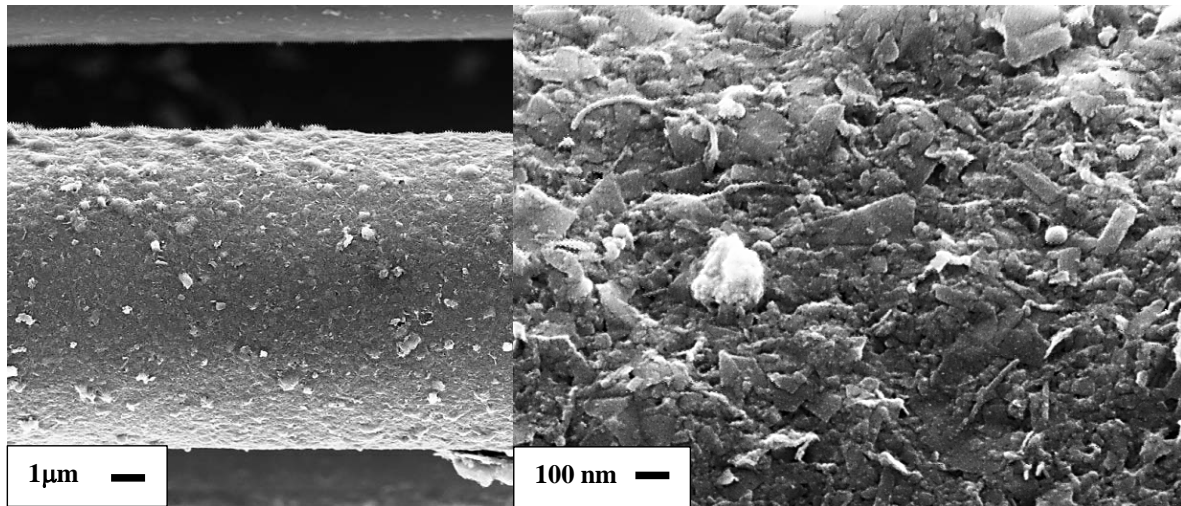


Figure 1: Example of an electrophoretically deposited coating of graphitic nanoplatelets (GNPs) on an E-glass fiber in which the GNPs were prepared using the ultrasonicated ozone process.

2 EXPERIMENTAL

2.1 Materials and Processing

Multi-walled CNTs (Hanwha Nanotech, Korea) were functionalized with ozone and polyethyleneimine (PEI) dendrimer (Sigma Aldrich, USA) under ultrasonication to produce a stable 1g/L aqueous dispersion [21, 22]. PEI was added at 1g/L to the ozone treated CNT solution and adjusted to a pH of 6 with acetic acid, facilitating the development of a positive surface charge required for EPD.

Borosilicate glass (Fisher Scientific, USA) was treated using γ -aminopropyltriethoxysilane (APS) for the preparation of model interphases. EPON 862 epoxy and its curing agent Epikure W (Momentive Specialty Chemicals Inc.) were mixed at a ratio of 100:26.4 to create the model interphase system. Samples were cured at 130°C for 6 hours under vacuum to replicate the VARTM process used to make the original glass/epoxy laminates [22].

Single E-glass fibers were separated from E-glass tows separated from a unidirectional non-woven fiber sheet (style 7721, 203 g/m², APS sizing, Thayercraft Inc., USA). A low viscosity bisphenol-A/F based epoxy resin DER 353 (Dow Chemical Company) and a bis (p-aminocyclohexyl) methane (PACM-20, Air Products and Chemicals, Inc.) curing agent were mixed at weight ratio of 100:28 to form microdroplets on the fibers. The resin were allowed to gel at room temperature first for 5 h followed by a cure cycle of 2h at 80°C then post cure of 2h at 150°C. Optical microscope pictures were taken to measure the droplet size and shape, fiber diameter, fiber embedded length, and fiber gage length.

2.2 Sample Preparation

2.2.1 Model Interphase

Figure 2 shows the configuration of preparing the model interphase specimens. Planar glass slides were first cleaned with plasma (PICO Low Pressure Plasma System P100, Diener Electronic GmbH) before applying any treatments. APS treatment was applied followed by a layer of ozone-PEI functionalized CNT film dropped onto the glass slides. The treated glass slides were dried at 110°C for 1 h after drying at room temperature overnight to represent the EPD process.

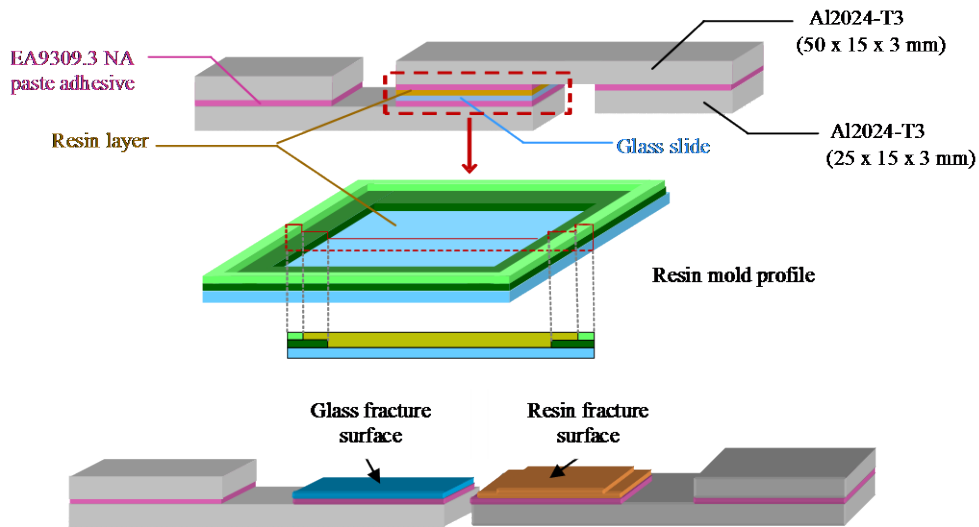


Figure 2: The configuration of the test specimen used for measuring the shear strength of the glass/resin model system. The respective fracture surfaces are shown corresponding to the surface with “glass” and “resin” appearance.

After completing the surface treatments, layers of tape were used to build a reservoir to hold the epoxy resin. The cured resin film and exterior glass surface were plasma cleaned and bonded to the aluminum adherends using an epoxy adhesive (EA93039.3 NA; Henkel, USA) to produce the lap shear test specimens.

2.2.2 Single Fiber Deposition

Single E-glass fibers were vertically aligned and taped onto isolated window frames under slight tension, as shown in Figure 3. Sandwiched single fibers were pressed onto the cathode side to ensure an intimate contact between the fibers and the stainless steel electrode. Teflon spacers were used to help maintain a consistent electrode separation distance. The entire fixture was vertically immersed in the CNT solution and deposition was conducted using a field strength of 64 V/cm for 12 minutes.

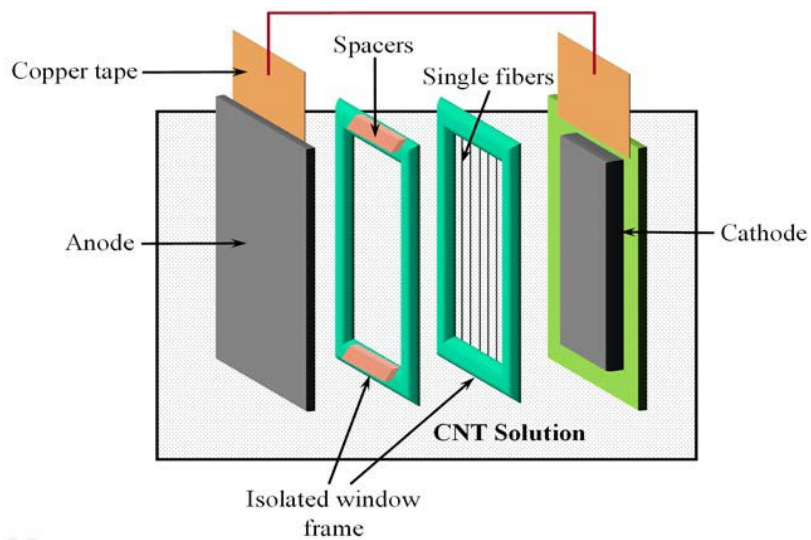


Figure 3: Schematic of single fiber setup for electrophoretic deposition.

2.3 Mechanical Characterization

2.3.1 Model Interphase

A custom-built tensile tester was used to test the shear strengths of the model interphases with a tensile extension rate of 1.5 mm/min. The peak shear stress at the maximum load was calculated from the closed form solution, which accounted for overlap distance and adherend stiffness [22]. In each treatment category, 5 to 10 specimens were tested and the mean strength and 95% confidence limit were determined.

2.3.2 Microdroplet Test

An epoxy drop was applied to each E-glass fiber with or without CNT-EPD coatings. After the epoxy resin drop was cured, the specimens were mounted onto glass rods and tested using a customized setup established by Gao [4], which consisted of an actuator driven load frame (Newport ESP 300 and Newport LTA-HS), using an open pan balance (Mettler Toledo PB303-S) as the load cell. Adjustable micro-knives were precisely positioned above the droplet and then moved into contact with the glass fiber as shown in Figure 4. Displacement of the fiber at a rate of 0.001 mm/s then resulted in the droplet reacting against the micro-knives and leading to shear pull-out of the fiber. Figure 6 shows a typical force-displacement curve. Due to variable failure modes a significant number of tests was required to achieve a significant dataset in which shear pull-out occurred.

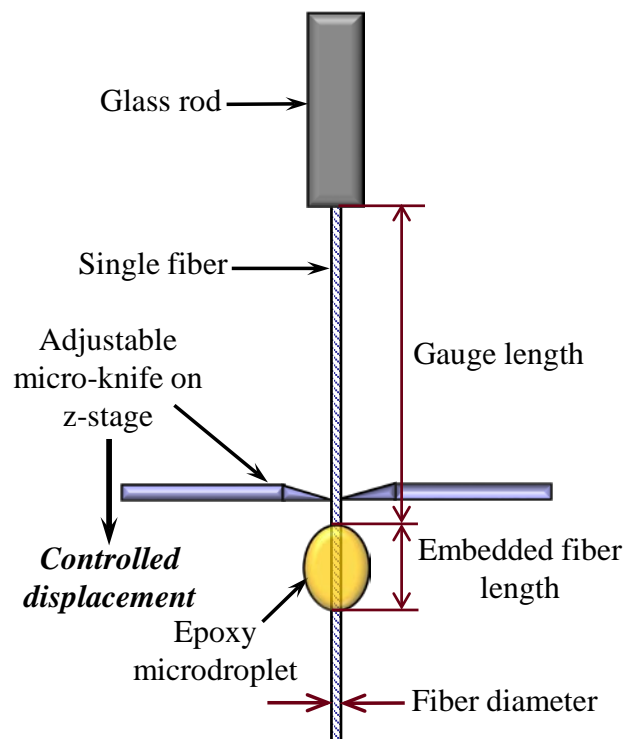


Figure 4: Schematic of microdroplet test setup and definition.

2.4 Chemical Characterization and Microscopy

XPS (Kratos Nova, UK) was used to characterize the chemical treatments and shear fracture surfaces, using monochromated Al $K_{\alpha,1}$ to illuminate an analysis area of $700 \times 300 \mu\text{m}^2$. Survey and region spectra were acquired with 160 eV and 20 eV pass energies, respectively. Calculated atomic concentrations typically had an error of $\pm 10\%$ of the measured value. Fracture specimens were analyzed using a field emission scanning electron microscope (AURIGA 60 Crossbeam FIB-SEM) operating at 3 kV with a sputter deposited Pt/Au layer to prevent charging.

3 RESULTS AND DISCUSSION

3.1 Model Interphase

3.1.1 Interfacial Shear Strength

Figure 5 shows the maximum shear stress measured for the glass-resin joints using APS treatments followed by deposition of the ozone and ozone-PEI functionalized CNTs. The peak shear stress of the APS treated specimens improved 23% compared to the plasma treated specimens. Introducing ozone functionalized CNTs lead to no further improvements but with a greater stress variation. However, a 50% increase over the baseline plasma treated samples was produced with the addition of ozone and PEI-functionalized CNTs. The shear results from the model interphase tests show a similar trend to that observed with the glass/epoxy composite laminates [22]. This increase in interfacial shear strength contributes to increases in the mechanical strength observed in the glass/epoxy laminates.

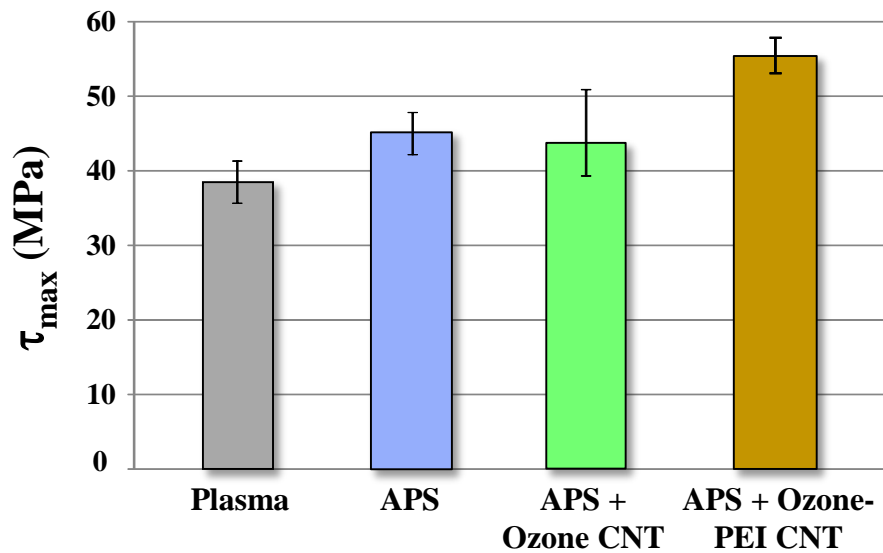


Figure 5: Maximum shear stress measured for model glass-resin joints in which plasma-treated glass substrates were treated with APS followed by deposition of ozone-CNTs and ozone-CNTs plus PEI.

3.1.2 Chemical Characterization

XPS was used to analyze each of the components used in the fabrication of the model glass-resin system and all fracture surfaces to better understand the influence of the CNT functionalization, glass surface chemistry and aqueous dispersion quality on the mechanical performance. Atomic concentrations of each analyzed surface were obtained and calculated from wide scan spectra. Individual C 1s, O 1s, N 1s and Si 2p spectra were collected for both glass and resin fracture surfaces of specimens with a high and low shear strength, as shown in Figure 2. In the case of low shear strength samples, the EPD solution was adjusted to a high pH level to deliberately destabilize the dispersion during film formation. Table 1 shows the elemental compositions and the C 1s chemical components for the strong and weak joints. It can be seen that the strong joint exhibits low levels of silicon (from glass or APS) and higher C sp^2 concentrations (from CNTs and epoxy) on the glass fracture side, when compared to the weak joint. This is indicative of fracture deeper into the CNT-rich interphase region in the strong joint and suggests the efficient dispersion and functionalization of the CNTs with PEI facilitate a stronger, more ductile interphase region. In contrast if the CNTs agglomerate, as was the case for the weak joint, fracture propagates close to the glass/matrix interface and the benefit of the CNT addition is reduced. In Section 3.3 SEM images of the fracture surfaces are discussed and confirm the XPS findings.

FAILURE SIDE	ATOMIC CONCENTRATION (%)								
	C=C	C-C	C-O/ C-N	C=O/ C=N	COO/ NCO	C	O	N	Si
Resin-strong	16.5	4.7	44.4	3.6	4.0	73.7	6.9	18.1	0.3
Glass-strong	6.0	9.1	42.5	4.7	2.5	65.3	12.1	18.2	3.9
Resin-weak	6.6	1.9	45.9	2.0	4.2	72.8	6.7	19.5	0.2
Glass-weak	3.5	8.4	49.7	4.3	5.9	42.0	30.1	12.7	11.5

Table 1: The XPS atomic concentrations measured for APS treated glass coated with ozone and PEI-functionalized CNTs after shear fracture indicating elemental compositions for the resin and glass surfaces for weak and strong joints.

3.2 Microdroplet Test

The interfacial properties of CNT-EPD coated E-glass fibers embedded in epoxy resin were analyzed and compared with baseline fiber specimens using the microdroplet test. In order to have a successful test, the specimen should fail through the fiber-droplet interface and before fiber tensile failure takes place. A typical force-displacement response from the microdroplet test of CNT EPD coated E-glass/epoxy specimen with an embedded fiber length of 117 μm is presented in Figure 6. The force-displacement plot initially increases almost linearly under elastic loading. During load application, the fiber deforms elastically. At higher loads interfacial crack initiation occurs. Complete debonding corresponds to point just after the maximum force (F) is reached, followed by a sudden load drop. Once complete debonding occurs, the fiber elastically relaxes and the load recorded corresponds to frictional stress generated by the dynamic sliding of the resin droplet over the glass fiber, which is strongly influenced by the fiber coating and texture.

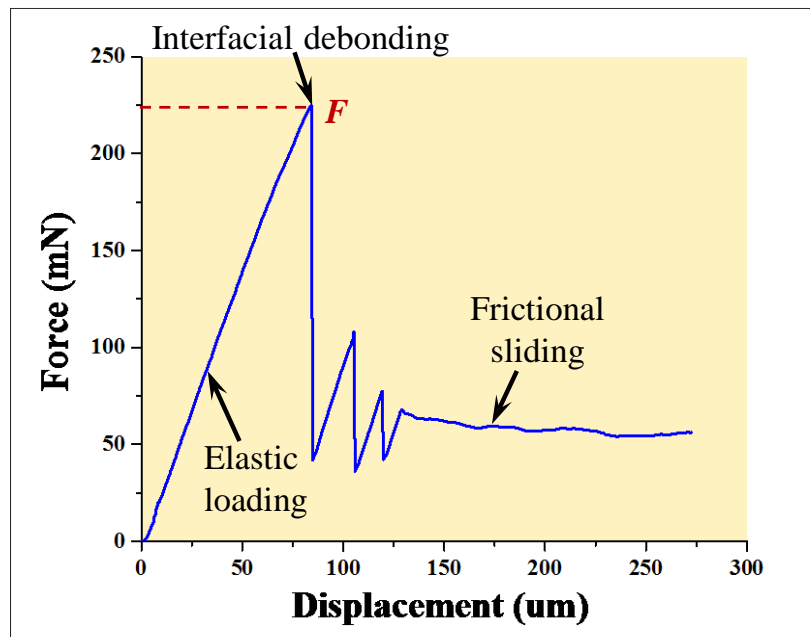


Figure 6: Typical force-displacement curve for a resin micro-droplet debonding from a CNT EPD coated E-glass fiber.

Preliminary results show the difference in the fiber embedded length does not influence the final interfacial shear strength and significant improvements can be achieved for the CNT-EPD coated fibers in comparison with only APS sized fiber specimens. This is in good agreement with prior results from the glass/epoxy composites and the model interphase study discussed in Section 3.1. Glass/epoxy composites exhibited an 80% improvement in in-plane shear strength corresponding to a 15% volume fraction of EPD-CNTs compared to the baseline laminate. In the model interphase study the addition of PEI-functionalized CNTs improved the toughness of the interphase region and led to both homogeneous fracture in the nanotube-rich interphase and 50% higher adhesion strength.

The increased interfacial shear strength of the CNT coated E-glass fiber may be attributed to the change in surface roughness and morphology created by the CNTs, providing opportunities for mechanical interlocking between fiber and resin as well as increased surface area for formation of chemical bonds between the CNTs, fiber and matrix. It is important to note that the silane based sizing chemistry for glass fiber system is already well developed and that the interfacial shear strength value for commercially sized E-glass fiber is of the order of 40 MPa, which is already 35% higher than unsized E-glass fibers (26 ± 3 MPa) [25].

3.3 Failure Mode Analysis

Figure 7 shows SEM images of fracture surfaces from the model interphase tests conducted in Section 3.1 and microdroplet testing in Section 3.2. The results indicate clear differences between strong and weak interphases. Figure 7(a) shows a flat glass surface with a low concentration of CNTs

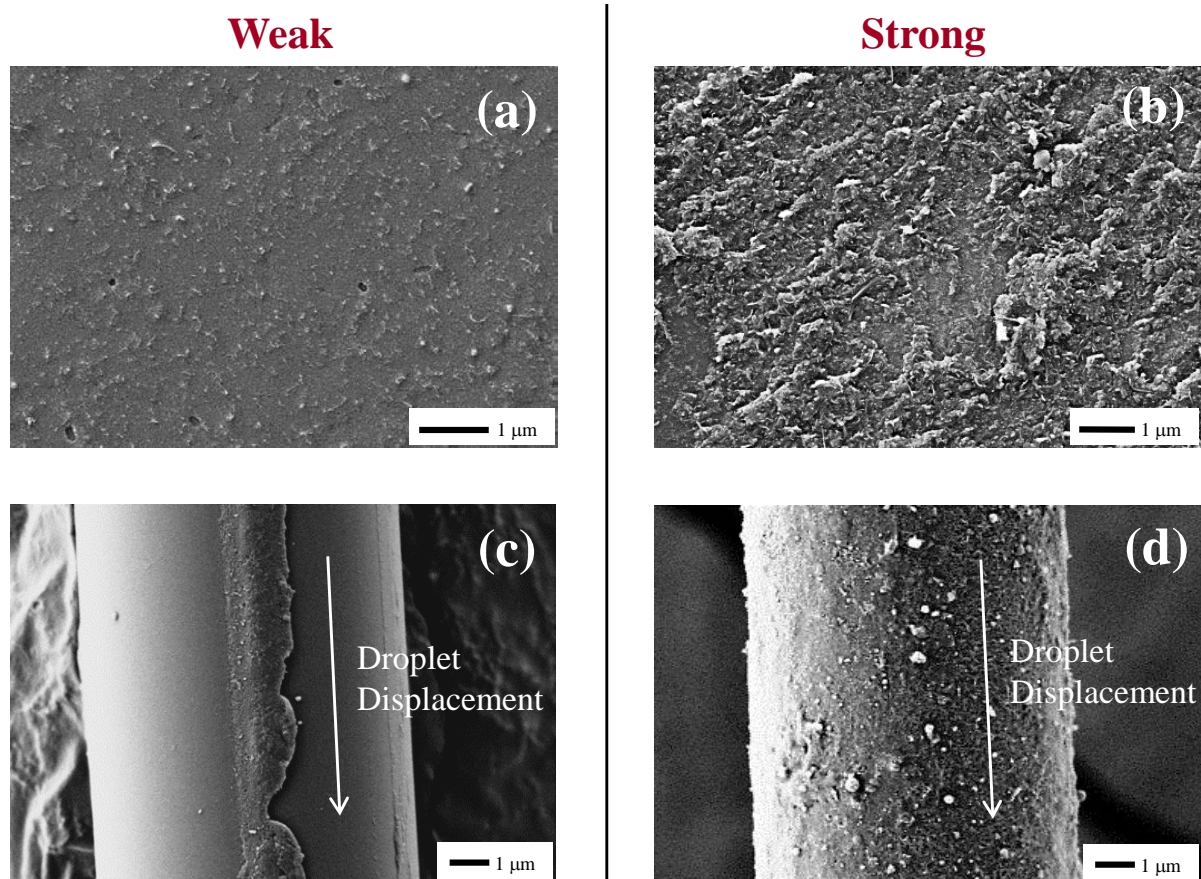


Figure 7: SEM images of model interphase glass-side fracture surfaces with (a) lower interfacial shear stress and (b) higher interfacial shear stress, and the sliding area of the microdroplet fracture specimens for CNT EPD coated fibers with (c) lower and (d) higher interfacial shear strength.

which resulted in a low shear strength. In contrast, Figure 7(b) shows the higher strength shear joint has a thicker covering of functionalized CNTs with the infused resin, confirming the XPS analysis (Table 1), which indicated higher shear strength corresponds to fracture in the CNT-rich interphase region. Similarly, in Figure 7(c) and 7(d) the micro-droplet test shows a contrasting fracture morphology for the weak and strong interphases, respectively. Figure 7(c) shows only a thin slice of CNTs in the droplet displacement direction, with the remaining area indicating a smooth, featureless surface. Figure 7(d) shows the strong microdroplet fracture surface with a rough morphology over the whole sliding area, characterized by a complete coverage of resin infused CNTs. These SEM images support the conclusion that when shear fracture propagates through the CNT-rich interphase layer, higher interfacial shear strength will result.

4 CONCLUSIONS

Electrophoretic deposition was successfully applied to coat single E-glass fibers with PEI-ozone functionalized CNTs to facilitate microdroplet testing of glass/epoxy interphases. Interphase characterization conducted by both model interphase studies using planar glass substrates and single fiber microdroplet tests, show increased interfacial shear strength with the PEI-functionalized CNT treatments. Integration of CNTs into the interphase region moves fracture away from the glass fiber surface and is believed to be responsible for the increased shear strength. Ultrasonic ozone treatment of CNTs provides a stable dispersion which enables chemical functionalization with PEI. The PEI dendrimer is critical in providing a chemical link between the CNTs and the matrix or fiber surface and improving the ductility of the interphase region.

ACKNOWLEDGEMENTS

The authors gratefully acknowledge the funding support from University of Delaware Graduate Student Office Fellowship Award and National Science Foundation (Grant CMMI-1254540: Dr. Mary Toney, Program Director).

REFERENCES

- [1] Drzal L, Madhukar M. Fibre-matrix adhesion and its relationship to composite mechanical properties. *J Mater Sci* 1993;28(3):569-610.
- [2] Berg J, Jones F. The role of sizing resins, coupling agents and their blends on the formation of the interphase in glass fibre composites. *Composites Part A: Applied Science and Manufacturing* 1998;29(9):1261-1272.
- [3] Mäder E, Jacobasch H, Grundke K, Gietzelt T. Influence of an optimized interphase on the properties of polypropylene/glass fibre composites. *Composites Part A: Applied Science and Manufacturing* 1996;27(9):907-912.
- [4] Gao X, Jensen R, McKnight S, Gillespie J. Effect of colloidal silica on the strength and energy absorption of glass fiber/epoxy interphases. *Composites Part A: Applied Science and Manufacturing* 2011;42(11):1738-1747.
- [5] Godara A, Gorbatiikh L, Kalinka G, Warriier A, Rochez O, Mezzo L, Luizi F, van Vuure AW, Lomov SV, Verpoest I. Interfacial shear strength of a glass fiber/epoxy bonding in composites modified with carbon nanotubes. *Composites Sci Technol* 2010;70(9):1346-1352.
- [6] Gao L, Thostenson ET, Zhang Z, Chou T. Sensing of Damage Mechanisms in Fiber-Reinforced Composites under Cyclic Loading using Carbon Nanotubes. *Advanced Functional Materials* 2009;19(1):123-130.
- [7] Li J, Wu Z, Huang C, Li L. Multiscale carbon nanotube-woven glass fiber reinforced cyanate ester/epoxy composites for enhanced mechanical and thermal properties. *Composites Sci Technol* 2014;104(0):81-88.
- [8] An F, Lu C, Li Y, Guo J, Lu X, Lu H, He S, Yang Y. Preparation and characterization of carbon nanotube-hybridized carbon fiber to reinforce epoxy composite. *Mater Des* 2012;33(0):197-202.
- [9] Zare Y. Effects of interphase on tensile strength of polymer/CNT nanocomposites by Kelly-Tyson theory. *Mech Mater* 2015;85(0):1-6.

- [10] Pavia F, Curtin WA. Molecular modeling of cracks at interfaces in nanoceramic composites. *J Mech Phys Solids* 2013;61(10):1971-1982.
- [11] Ireland R, Arronche L, La Saponara V. Electrochemical investigation of galvanic corrosion between aluminum 7075 and glass fiber/epoxy composites modified with carbon nanotubes. *Composites Part B: Engineering* 2012;43(2):183-194.
- [12] Rahmanian S, Suraya AR, Shazed MA, Zahari R, Zainudin ES. Mechanical characterization of epoxy composite with multiscale reinforcements: Carbon nanotubes and short carbon fibers. *Mater Des* 2014;60(0):34-40.
- [13] Aguilar Ventura I, Lubineau G. The effect of bulk-resin CNT-enrichment on damage and plasticity in shear-loaded laminated composites. *Composites Sci Technol* 2013;84(0):23-30.
- [14] Bekyarova E, Thostenson ET, Yu A, Kim H, Gao J, Tang J, Hahn HT, Chou T-, Itkis ME, Haddon RC. Multiscale carbon nanotube-carbon fiber reinforcement for advanced epoxy composites. *Langmuir* 2007;23(7):3970-3974.
- [15] Lee S-, Choi O, Lee W, Yi J-, Kim B-, Byun J-, Yoon M-, Fong H, Thostenson ET, Chou T-. Processing and characterization of multi-scale hybrid composites reinforced with nanoscale carbon reinforcements and carbon fibers. *Composites Part A: Applied Science and Manufacturing* 2011;42(4):337-344.
- [16] Boccaccini AR, Cho J, Roether JA, Thomas BJC, Jane Minay E, Shaffer MSP. Electrophoretic deposition of carbon nanotubes. *Carbon* 2006;44(15):3149-3160.
- [17] Peng K, Liu L-, Li H, Meyer H, Zhang Z. Room temperature functionalization of carbon nanotubes using an ozone/water vapor mixture. *Carbon* 2011;49(1):70-76.
- [18] Li M, Boggs M, Beebe TP, Huang CP. Oxidation of single-walled carbon nanotubes in dilute aqueous solutions by ozone as affected by ultrasound. *Carbon* 2008;46(3):466-475.
- [19] Shaffer MSP, Fan X, Windle AH. Dispersion and packing of carbon nanotubes. *Carbon* 1998;36(11):1603-1612.
- [20] Sham M-, Kim J-. Surface functionalities of multi-wall carbon nanotubes after UV/Ozone and TETA treatments. *Carbon* 2006;44(4):768-777.
- [21] An Q, Rider AN, Thostenson ET. Electrophoretic deposition of carbon nanotubes onto carbon-fiber fabric for production of carbon/epoxy composites with improved mechanical properties. *Carbon* 2012;50(11):4130-4143.
- [22] An Q, Rider AN, Thostenson ET. Hierarchical composite structures prepared by electrophoretic deposition of carbon nanotubes onto glass fibers. *ACS applied materials & interfaces* 2013;5(6):2022-2032.
- [23] Rider A, An Q, Thostenson E, Brack N. Ultrasonicated-ozone modification of exfoliated graphite for stable aqueous graphitic nanoplatelet dispersions. *Nanotechnology* 2014;25(49):495607.
- [24] Rider AN, An Q, Brack N, Thostenson ET. Polymer nanocomposite – fiber model interphases: Influence of processing and interface chemistry on mechanical performance. *Chem Eng J* 2015;269(0):121-134.
- [25] Andres Leal A, Deitzel JM, McKnight SH, Gillespie Jr. JW. Interfacial behavior of high performance organic fibers. *Polymer* 2009;50(5):1228-1235.